Piezoelectric ZnO Thin Films for 2DOF MEMS Vibrational Energy Harvesting

Kai Tao[1], Haiping Yi[1], Lihua Tang[2], Jin Wu[3*], Peihong Wang[4], Nan Wang[5], Liangxing Hu[5], Yongqing Fu[6], Jianmin Miao[5*] and Honglong Chang[1*]

[1]Ministry of Education Key Laboratory of Micro and Nano Systems for Aerospace, Northwestern Polytechnical University, Xi'an 710072, PR China

[2]Department of Mechanical Engineering, University of Auckland, 20 Symonds Street, Auckland 1010, New Zealand

[3]State Key Laboratory of Optoelectronic Materials and Technologies and the Guangdong Province Key Laboratory of Display Material and Technology, School of Electronics and Information Technology, Sun Yat-sen University, Guangzhou 510275, PR China

[4]School of Physics & Materials Science, Anhui University, Hefei 230601, PR China

[5]School of Mechanical and Aerospace Engineering, Nanyang Technological University, 50 Nanyang Avenue, 639798 Singapore

[6]Faculty of Engineering and Environment, Northumbria University, Newcastle upon Tyne, NE1 8ST, UK

E-mail: wujin8@mail.sysu.edu.cn; mjmmiao@ntu.edu.sg; changhl@nwpu.edu.cn

Abstract. Zinc oxide (ZnO) is an environmental-friendly semiconducting, piezoelectric and non-ferroelectric material, and plays an essential role for applications in microelectromechanical systems (MEMS). In this work, a fully integrated two-degree-of-freedom (2DOF) MEMS piezoelectric vibration energy harvester (p-VEH) was designed and fabricated using ZnO thin films for converting kinetic energy into electrical energy. The 2DOF energy harvesting system comprises two subsystems: the primary one for energy conversion and the auxiliary one for frequency adjustment. Piezoelectric ZnO thin film was deposited using a radio-frequency magnetron sputtering method onto the primary subsystem for energy conversion from mechanical vibration to electricity. Dynamic performance of the 2DOF resonant system was analyzed and optimized using a lumped parameter model. Two closely located but separated peaks were achieved by precisely adjusting mass ratio and frequency ratio of the resonant systems. The 2DOF MEMS p-VEH chip was fabricated through a combination of laminated surface micromachining process, double-side alignment and bulk micromachining process. When the fabricated prototype was subjected to an excitation acceleration of 0.5 g, two close resonant peaks at 403.8 and 489.9 Hz with comparable voltages of 10 and 15 mV were obtained, respectively.

Submitted to: *Surface & Coatings Technology*

1. Introduction

Recent advances in internet of things (IoT) and wireless sensing networks provide new insights into sustainability and availability of new types of micro-energy storage and conversion devices, including MEMS-based micro/nano generators, thermoelectrics and solar cells [1-3]. Conventional MEMS-based vibration energy harvesters are capable of transforming mechanical energy into electrical energy through piezoelectric [4-6], electromagnetic [7-9], electrostatic [10-12] and triboelectric mechanisms [13-15]. Piezoelectric materials possess a unique merit of direct electromechanical coupling which can efficiently convert mechanical strain into electrical energy and vice versa. MEMS-based piezoelectric vibration energy harvesters (p-VEH) have advantages of high power density and ease of miniaturization. Therefore, MEMS p-VEH is capable of converting kinetic energy into electrical energy by continuously pre-stressing or stretching piezoelectric materials under external cyclic loadings.

Generally the performance of p-VEHs is highly dependent on the piezoelectric properties of the materials. The piezoelectric materials commonly used for actuating and sensing include piezo-ceramics such as lead zirconate titanate (PZT), barium titanate ($BaTiO_3$), single crystal of quartz, thin films of ZnO or AlN, as well as thick films based on piezoceramic powders and polymeric materials (PVDF). Though the piezoceramics including PZT and micro-fiber-composites (MFC) are the common choices as the transducers for energy harvesting applications, they encounter difficulties in miniaturization, thin film deposition, and MEMS fabrication process [16], which make them non-applicable in micro-scale applications. PVDF is a semicrystalline polymer that exhibits the largest piezoelectric constants among piezo-polymers. However, PVDF encounters challenge to form uniform β phase crystal orientation during the silicon-based spin-coating process, making them more suitable in wearable and flexible applications. $BaTiO_3$ thin films have relatively high piezoelectric coefficient and high dielectric properties. The high temperature annealing process for crystallization is a challenge for MEMS compatible multilayered fabrication process. Both AlN and ZnO are lead-free environmental-friendly non-ferroelectric materials. They have excellent semiconducting and piezoelectric properties with permanent polarizations along the c-axis crystallographic direction. AlN has been widely used in energy harvesting and ultrasound tweezers applications [17-19]. ZnO piezoelectric thin film does not require high-temperature post-deposition annealing and high-voltage poling process [20]. Due to these unique merits, ZnO-based piezoelectric thin film plays an essential role in MEMS applications including sensors [21], actuators [22] , acoustic wave generators [23, 24] and smart slider to detect the head-disk contact [25]. In this work, we integrate ZnO thin film into a MEMS p-VEH for converting ambient kinetic energy of vibrations to electrical energy.

For vibration-based MEMS energy harvesting applications, one of the key challenges is the narrow operation bandwidth [26]. The MEMS-based energy harvester is usually designed as a single spring-mass-damper (1DOF) system. The kinetic energy can only be scavenged near its intrinsic resonance frequency whereas the ambient vibrations usually have broadband frequency spectra or multiple peaks. To address this limitation, numerous approaches for frequency broadening have been proposed, including multimodal energy harvesting [27-29], resonance tuning [30] and other nonlinear techniques [31-33]. Multimodal energy harvesters are supposed to be more effective with matched multiple frequencies to better harness kinetic energy in these scenarios. For MEMS-based p-VEH energy harvesters, multimodal techniques are also more advantageous in terms of wafer-level fabrication and minimal post-assembly process.

This work presents design and fabrication of ZnO-based MEMS p-VEH with two-degree-of-freedom (2DOF) and multi-modal structure. The 2DOF system has a primary subsystem for energy conversion and an auxiliary subsystem for frequency adjustment, and piezoelectric ZnO thin film is deposited onto the primary subsystem for strain-to-electricity energy conversion.

2. Device Design and Fabrication

A schematic design of the proposed 2DOF MEMS p-VEH with ZnO thin films is shown in Figure 1. The 2DOF spring-mass resonant structure is constructed on a SiO_2/Si/SiO_2 wafer. It is composed of two subsystems. The inner auxiliary subsystem has a circular mass suspended by three parallel spiral beams. The diameter and height of the circular mass are 3.4 mm and 500 µm, respectively. The geometry of spiral beam is formed with three 120° circular arcs, which are designed with different radii and tangentially connected to each other at the conjunction points. The outer primary subsystem has a ring shape mass suspended by three small arc beams. The ring shape mass has an outer radius of 5.4 mm, an inner radius of 2.05 mm and a height of 500 µm. Each small arc beam has an outer radius of 5.75 mm, an inner radius of 5.5 mm and a height of 45 µm. The arc beams are evenly arranged in a rotatory symmetry with 120° distributed around the primary mass. It is worthwhile to note that the heights of both the outer and inner masses are the same as the wafer thickness of 500 µm, whereas the suspended beams are only 45 µm in height and made using a double-side deep reactive ion etching (DRIE) process. The low stiffness and large mass configuration will facilitate low resonances of the whole 2DOF system.

Piezoelectric ZnO thin film is deposited and patterned on the top of the outer arc beams for energy harvesting as shown in Figure 1. The ZnO thin film is sandwiched with top and bottom Pt/Au electrodes. Since ZnO is a non-ferroelectric material, the whole process can be conducted at room temperature and eliminate high-temperature post annealing and high-voltage poling processes. When an external vibration source excites the 2DOF spring-mass resonant structure, the ZnO thin film on the surface of outer arc beams will be continuously stressed and stretched, thus effectively converting the mechanical energy into electricity.

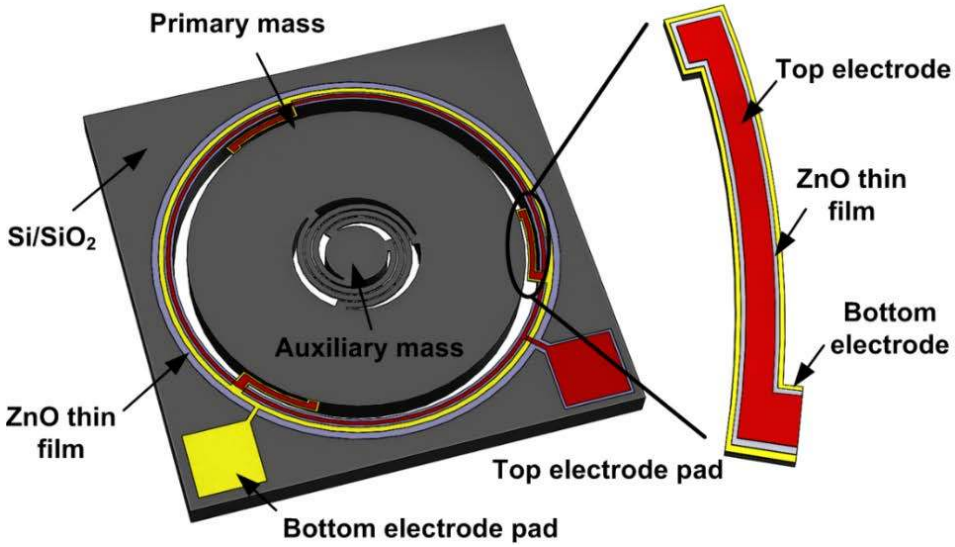

Figure 1. *Schematic illustration of 2DOF MEMS p-VEH chip and enlarged view of ZnO thin film sandwiched structure (top electrode layer/ZnO layer/bottom electrode layer)*

The fabrication procedure of the ZnO-based 2DOF MEMS p-VEH chip is shown in Figure 2. The procedures include a sacrificial layer-by-layer surface micromachining process and a double-side DRIE bulk micromachining process. It begins with a 500 μm thick SiO_2/Si/SiO_2 wafer substrate. Pt (150nm)/Au (150nm) conducting layer is patterned on top of SiO_2 insulation layer through a sputtering and lift-off process (Figure 2(a)). The Pt/Au layer is served as the bottom electrode. Photoresist is then spin coated on the surface of bottom electrode. This is followed by a lithography process to create windows for the next step of thin film deposition (Figure 2(b)). One of the critical processes is the room-temperature deposition of ZnO piezoelectric thin film, which was obtained by RF magnetron sputtering a 3 mm thick and 99.99% purity ZnO target (Figure 2(c)). After that, the ZnO is patterned using a wet etching process (Figure 2(d)). Another Pt (150nm)/Au (150nm) layer served as the top electrode is deposited onto the top of ZnO layer through the lift-off process as shown in Figure 2(b). Thus, the top electrode layer/ZnO layer/bottom electrode layer is formed with a sandwiched structure (Figure 2(e)). The following step is to define the 2DOF resonant structure. For this purpose, SiO_2 via is formed by photolithography and reactive-ion etching (RIE) process (Figure 2(f)). Subsequently, the DRIE process is applied to etch away the silicon substrate to pattern the front-side spring-mass structure (Figure 2(g)). The wafer is front-side bonded to another supporting wafer using a heat conductive silver paste and then backside etched using the DRIE process to form the seismic mass. Finally, the supporting wafer is removed and the whole ZnO-based 2DOF MEMS energy harvesting chip is released (Figure 2(f)).

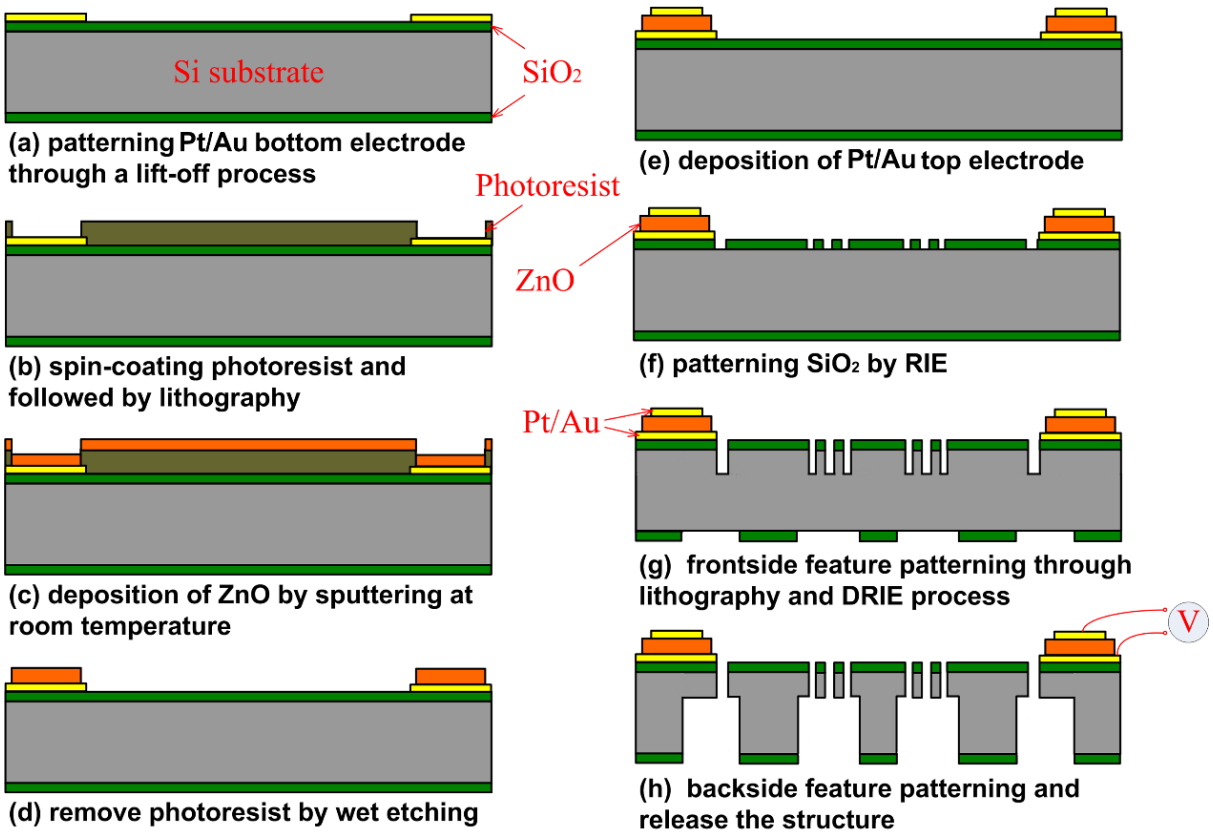

Figure 2. *Fabrication procedure of ZnO-based 2DOF MEMS p-VEH chip on SiO_2/Si/ SiO_2 wafers*

3. Modeling of 2DOF MEMS p-VEH

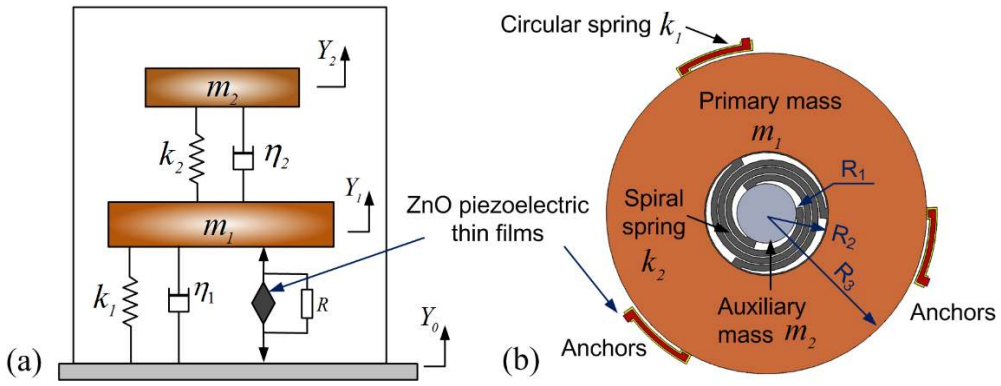

Figure 3. *(a) Lumped parameter model of proposed 2DOF MEMS p-VEH with ZnO piezoelectric thin film; (b) the corresponding 2DOF spring-mass resonant structure*

The lumped parameter model and the spring-mass resonant structure of proposed 2DOF MEMS p-VEH are shown in Figures 3(a) and 3(b), respectively. In this work, we aim to design the structure to provide two closely located and comparable resonant peaks so that the energy harvesting is more robust in the practical vibration scenarios. The primary subsystem of the 2DOF p-VEH has the primary mass m_1, mechanical damping η_1, spring stiffness k_1 and piezoelectric element. The auxiliary subsystem has the auxiliary mass m_2, mechanical damping η_2 and spring stiffness k_2. The governing equation of the 2DOF MEMS p-VEH system can be derived as:

$$\begin{cases} m_1\left(\ddot{Y}_1-\ddot{Y}_0\right)+\eta_1\left(\dot{Y}_1-\dot{Y}_0\right)+k_1\left(Y_1-Y_0\right)+\theta V-\eta_2\left(\dot{Y}_2-\dot{Y}_1\right)-k_2\left(Y_2-Y_1\right)=-m_1\ddot{Y}_0 \\ m_2\left(\ddot{Y}_2-\ddot{Y}_1\right)+\eta_2\left(\dot{Y}_2-\dot{Y}_1\right)+k_2\left(Y_2-Y_1\right)=-m_2\ddot{Y}_1 \end{cases} \tag{1}$$

where θ is the electromechanical coupling coefficient; V is the voltage across the load resistance R; θV is the backward electromechanical coupling force (θV) induced by piezoelectric thin film. In the piezoelectric energy harvesters (p-VEH), the dynamic behavior is generally dominated by spring restoring force, backward electromechanical coupling force and other mechanical damping forces. In the current study, the backward electromechanical coupling force (θV) induced by ZnO thin films is much smaller than the spring restoring force due to the low piezoelectric coefficient and small ZnO thin film thickness. Considering the weak coupling conditions in the current energy conversion system, the effect of the backward electromechanical coupling force (θV) on the dynamic behavior of the 2DOF system is negligible. The main objective of the modeling is to reveal the mechanism that two comparable and close peaks can be achieved by carefully controlling spring-mass parameters. These phenomena can also predicted by the dimensionless displacement of the primary mass. Therefore, the piezoelectric backward force (θV) is not taken into account in the current study. Therefore, assuming $x = Y_1 - Y_0$ and $y = Y_2 - Y_1$ and rearranging equation (1), we now obtain:

$$\begin{cases} \left(m_1+m_2\right)\ddot{x}+\eta_1\dot{x}+k_1x+m_2\ddot{y}=-\left(m_1+m_2\right)\ddot{Y}_0 \\ m_2\ddot{y}+\eta_2\dot{y}+k_2y=-m_2\ddot{x}-m_2\ddot{Y}_0 \end{cases} \tag{2}$$

The following dimensionless parameters have been defined as:

$$\omega_1=\sqrt{\frac{k_1}{m_1}},\ \ \omega_2=\sqrt{\frac{k_2}{m_2}},\ \ \zeta_1=\frac{\eta_1}{2\sqrt{k_1m_1}},\ \ \zeta_2=\frac{\eta_2}{2\sqrt{k_2m_2}},\ \ \mu=\frac{m_2}{m_1},\ \ \alpha=\frac{\omega_2}{\omega_1},\ \ \Omega=\frac{\omega}{\omega_1} \tag{3}$$

Applying Laplace Transform, equation (2) can be modified into:

$$\begin{cases}(1+\mu)s^2\hat{X}+2\zeta_1\omega_1 s\hat{X}+\omega_1^2\hat{X}+\mu s^2\hat{Y}=-(1+\mu)s^2\hat{Y}\\ s^2\hat{Y}+2\zeta_2\omega_2 s\hat{Y}+\omega_2^2\hat{Y}=-s^2\hat{X}-s^2Y_0\end{cases} \tag{4}$$

where μ, α and ζ are the dimensionless parameters representing the mass ratio, frequency tuning ratio and the damping ratio, respectively; ω_1 and ω_2 are the natural frequencies of the primary and auxiliary subsystems, respectively. By solving equation (4) and applying $s=j\omega$, the dimensionless displacement of the primary mass can be obtained as

$$\left|\tilde{X}\right|=\left|\frac{\Omega^2\left(1+\mu-\dfrac{\Omega^2}{\alpha^2+j2\zeta_2\alpha\Omega}\right)}{1-(1+\mu)\Omega^2+j2\zeta_1\Omega+\dfrac{\Omega^4-\Omega^2-j2\zeta_1\Omega^3}{\alpha^2+j2\zeta_2\alpha\Omega}}\right| \tag{5}$$

In order to achieve two closely located and comparable resonant peaks, the mass ratio (μ) and frequency tuning ratio (α) should be carefully adjusted in the model. Figure 4 shows the contour plot of normalized displacements of the primary mass versus different mass ratios (μ) and frequency tuning ratios (α) under various excitation frequencies (Ω): (a) α=0.8; (b) α=0.9; (c) α=1.0; (d) α=1.1. The primary damping (ζ_1) and the auxiliary damping (ζ_2) are set to be 0.004. It can be seen that two peaks can be created with the proposed 2DOF resonant system. When the frequency tuning ratio (α) is around 0.9～1 and the mass ratio (μ) is tuned to be a very small value, two closely located and comparable peaks can be obtained as shown in Figures 4(b) and 4(c). In this work, α and μ are set to be 0.92 and 0.04, respectively. These form a theoretical foundation of the mechanical design of our proposed 2DOF spring-mass system. The details of the design parameters of proposed 2DOF MEMS p-VEH chip are listed in Table 1.

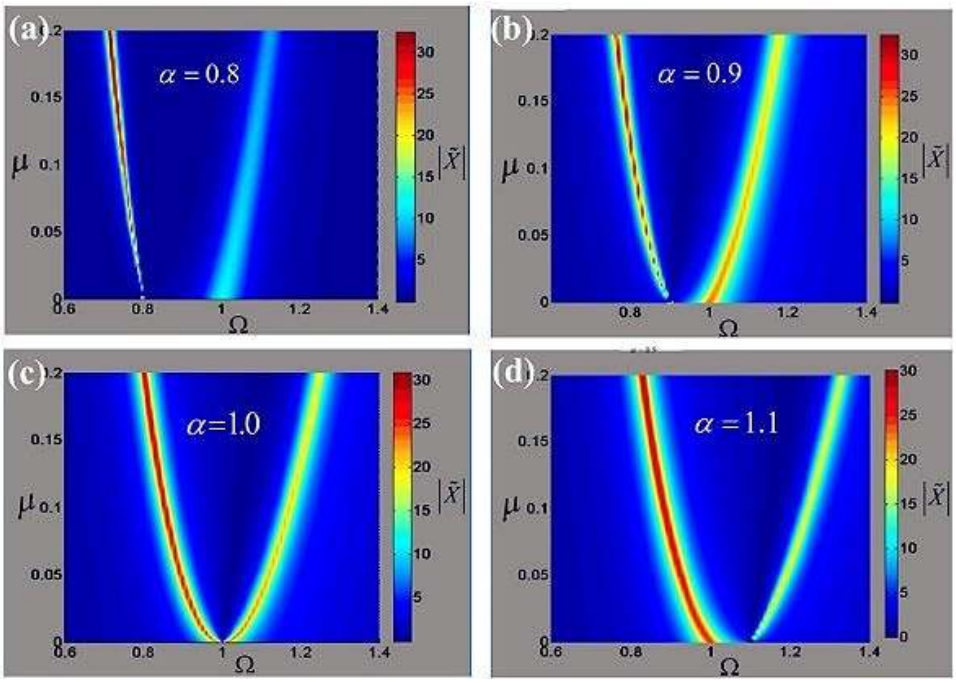

Figure 4. *Contour plotting of normalized displacement of the primary mass versus different mass ratios (μ) and frequency tuning ratios (α) under various excitation frequencies (Ω): (a) α=0.8; (b) α=0.9; (c) α=1.0; (d) α=1.1*

Table 1. *Design parameters of proposed 2DOF MEMS p-VEH chip*

Component	Designed parameter	Values
Primary mass	Height h_1	500 μm
	Radius R_1	1 mm
	Weight m_1	3.66 mg
Auxiliary mass	Outer radius R_3	5.4 mm
	Inner radius R_2	2.05 mm
	Weight m_2	91.3 mg
	Height h_2	500 μm
Outer spring beam	Height h_o	45 μm
	Circular arc angle θ	6.3°
	Inner radius R_4	5.5 mm
	Outer radius R_5	5.75 mm
Inner spring beam	Height h_i	45 μm
	Width w_i	200 μm
	Spacing l_i	50 μm
ZnO thin films	ZnO Thickness d_z	1.1μm
	Top Pt/Au d_t	300 nm
	Bottom Pt/Au d_t	300 μm
	Resistance R_i	240 kΩ
MEMS p-VEH chip	Volume V_o	14.5×14.5×0.5 mm^3

4. Results and Discussion

4.1 MEMS Device Characterization

Figure 5(a) shows the optical image of the fabricated 2DOF MEMS p-VEH chip. The overall size of the energy-harvester is 14.5 mm×14.5 mm×500 μm. It is observed that the surface color of the inner spiral beam and small circular mass becomes purple after the micromachining process. This is probably due to the local heating problem during the long-time DRIE process. SEM image of the inner auxiliary circular mass with parallel and spiral beams is shown in Figure 5(b). It can be seen that the surface of beam and mass is flat even though the thickness of the spiral beam is as thin as 43～45 μm. The top view of the sandwiched structure is shown in Figure 5(c), which was fabricated through a laminated layer-by-layer surface micromachining process. One of the key concerns is the short circuit problem of the top and bottom electrodes. Therefore, during the ZnO film deposition using the RF magnetron sputtering process, the bottom electrode was fully covered by the ZnO films. As shown in Figure 5(d), the line width of the top electrode is designed to be relatively narrow. Even though some misalignment could occur during the multilayer MEMS processes, the overall device is still safe to be operated effectively.

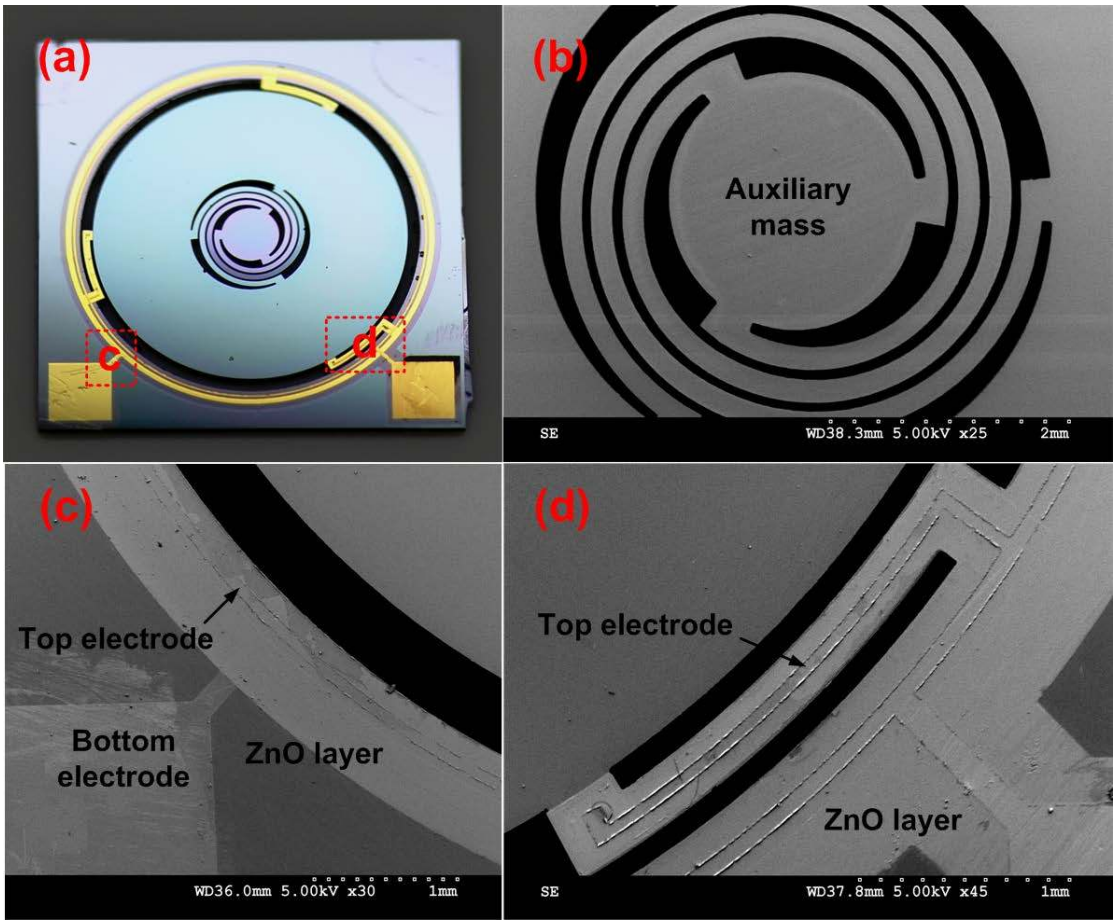

Figure 5. *(a) ZnO-based 2DOF p-VEH chip; (b) SEM images of the auxilliary mass with inner spiral beams; (c) top view of ZnO thin film with top electrode; (d) SEM images of the outer circular-spring beam with ZnO thin film and top electrode*

The cross-section morphology of ZnO-based multilayer thin film was characterized using a field-emission scanning electron microscope (FE-SEM), and the image is shown in Figure 6(a). It can be clearly observed that the ZnO thin film exhibits textured polycrystalline property with RF magnetron sputtering deposition process. The multilayer thin film structure can be clearly observed, including silicon substrate, SiO_2 insulation layer, bottom Pt/Au electrode layer, ZnO piezoelectric thin film layer and top Pt/Au electrode layer. The thickness values of the ZnO and SiO_2 are around 1.1 and 0.5 μm, respectively. The cross-sectional morphology clearly shows that the ZnO thin film has a uniform columnar structure which is perpendicular to the top surface. The crystal orientation of fabricated ZnO thin film was examined using X-ray diffraction (XRD), which shows that the ZnO thin film is highly c-axis-oriented (e.g., with a (0002) orientation in Figure 6(b)) and have an excellent piezoelectric quality. The piezoelectric coefficient of ZnO thin film by the current sputtering process is about 4.66 pC/N. The atomic composition ratio of the multilayered structure on the cross section of the multilayered structure was determined using energy dispersive X-ray spectroscope (EDS), and the result is shown in Figure 7. The atomic percentages of oxygen, silicon, zinc and platinum are 53.98, 26.48, 17.91 and 18.37 %, respectively. Gold layer may be covered by the ZnO film, therefore, gold atom was not detected in the EDS experiment. Clearly the EDS analysis is able to confirm that silicon oxide insulation layer, zinc oxide piezoelectric layer and platinum conducting layer all exist on the surface of the fabricated sample structure.

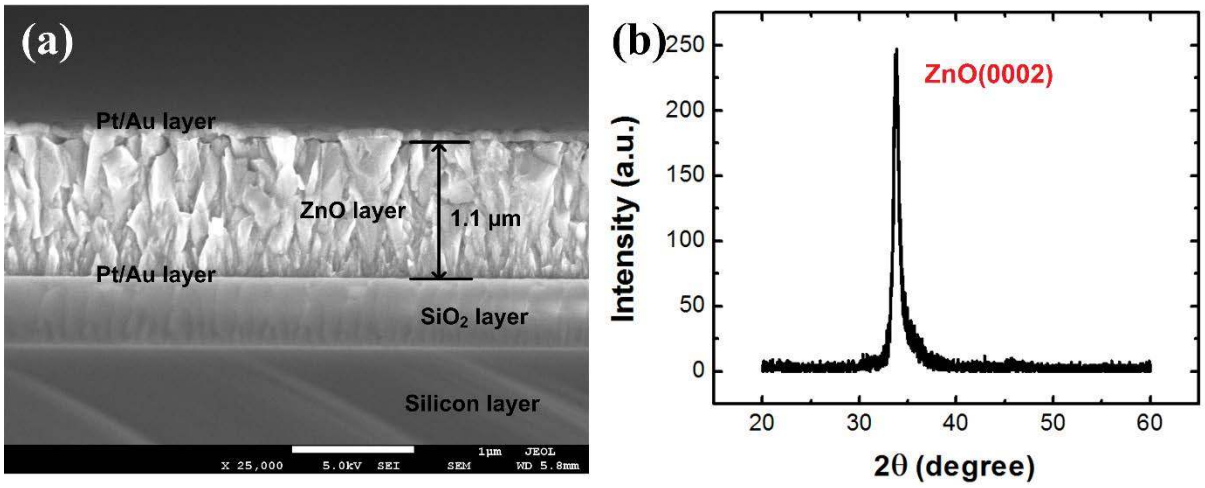

Figure 6. *(a) Cross-section FE-SEM image of multilayered structure of prototype: Pt/Au conducting layer, ZnO piezoelectric layer, SiO_2 insulating layer and silicon-supporting layer; (b) X-ray diffraction (XRD) pattern of the ZnO thin film*

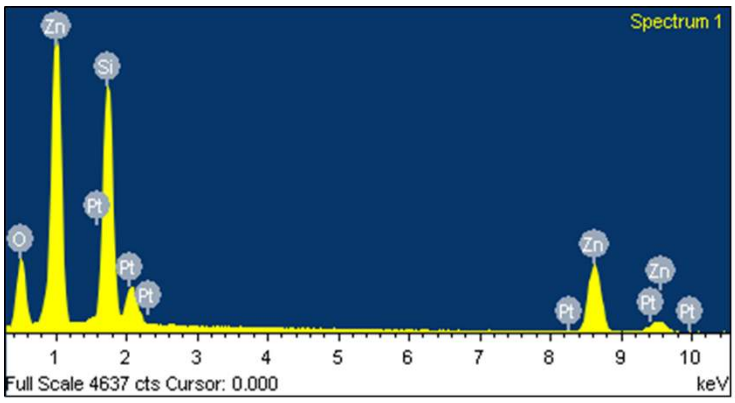

Cross-sectional energy dispersive X-ray spectroscopy spectrum analysis

Element	Weight %	Atomic %
O Kα (Oxygen)	27.91	53.98
Si Kα (Silicon)	24.03	26.48
Zn Kα (Zinc)	37.83	17.91
Pt Mα (Platinum)	10.23	1.62

Figure 7. *Energy dispersive X-ray spectroscope spectrum (EDS) of the piezoelectric multilayered structure*

4.2. Power Generation Experiment

The fabricated energy harvester was attached to a vibration testing system for its electrical performance evaluation. The testing setup was composed of a function generator, a voltage amplifier, an accelerometer, a shaker and a data acquisition system (DAQ NI USB-6289 M series). In the experiment, the excitation frequency was swept from 350 to 500 Hz at 0.5 g with a constant rate of 5 Hz/s and a load resistance of 250 kΩ was applied to the MEMS 2DOF p-VEH chip. Output voltage response in time-domain signal was directly recorded with the DAQ system, and the results are shown in Figure 8(a). It is noted that two comparable peaks have been obtained with the output voltages around 10 and 15 mV, respectively. This is consistent with the predicted results from the modeling (see Section 3) that two effective peaks can be obtained assuming $\alpha = 0.92$ and $\mu = 0.04$. After a fast Fourier transform (FFT) was applied to analyze the time-domain signal, the two resonant peaks are found to be 403.8 and 489.9 Hz, respectively, as shown in Figure 8(b). The frequency ratio of the second peak to the first one is only 1.21, which is superior to those reported in the literature [27, 28]. The output powers and voltages of the fabricated 2DOF p-VEH device at various load resistances are presented in Figure 9. The operating frequency and excitation acceleration were set to be 490 Hz and 0.5 g, respectively, during the measurement. The maximum output power is 0.46 nW with an optimal load resistance of 240 kΩ. The normalized power density of the p-VEH device, defined by power/volume/acceleration^2, was calculated to be 1.75×10^{-7} W•cm^{-3}•g^{-2} for the prototyped device. Although the performance of fabricated prototype is moderate at the current stage, it offers new insights in realizing 2DOF multimode MEMS energy harvester with piezoelectric ZnO thin films.

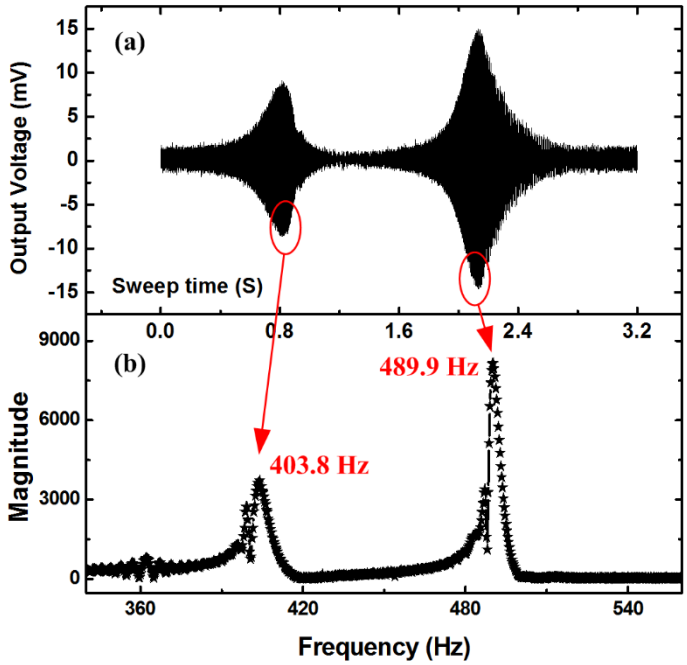

Figure 8. *Output voltage of the MEMS 2DOF p-VEH prototype with a swept frequency from 350 to 500 Hz: (a) output voltage in time domain response; (b) frequency domain signal by fast Fourier transform*

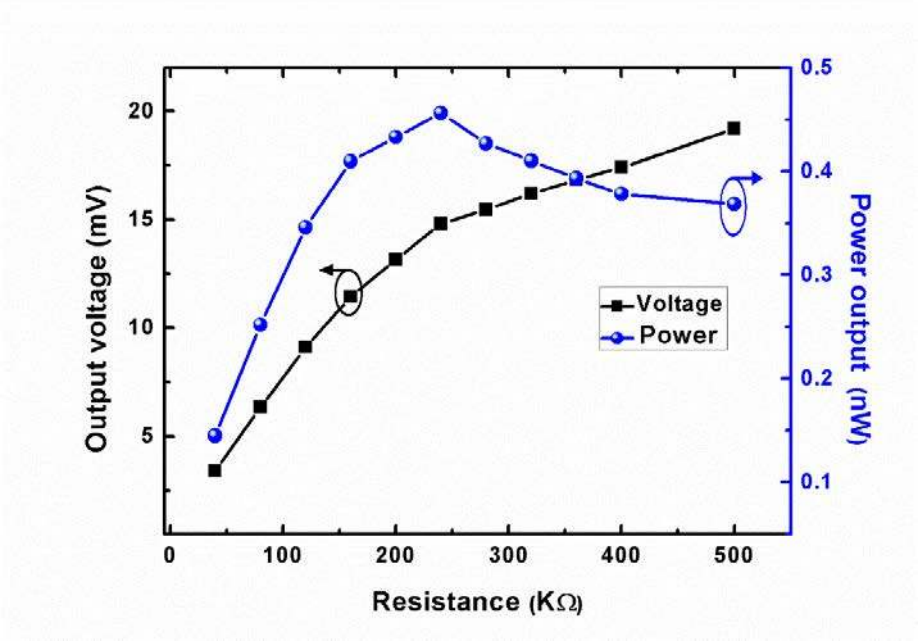

Figure 9. *Output voltages and powers against different resistances at the resonance of 490 Hz with the acceleration of 0.5g*

5. Conclusion

In this paper, a fully integrated MEMS 2DOF energy harvester based on ZnO thin films was successfully designed, modeled, fabricated and characterized. The MEMS p-VEH harvester with a volume of 14.5×14.5×0.5 mm^3 has a primary subsystem for energy conversion and an auxiliary subsystem for frequency adjustment. Through lumped parameter modeling and analysis, it was found by controlling

a frequency tuning ratio (α) of 0.9～1 and a mass ratio (μ) approximate 0, two closely located and comparable peaks can be obtained. The MEMS p-VEH chip was successfully fabricated using a laminated layer-by-layer surface micromachining process and double-side DRIE bulk micromachining process. The power generation capability of the fabricated energy harvester was characterized. Power generation experiment showed two closely located peaks at 403.8 and 489.9 Hz with comparable generated voltages of 10 and 15 mV, respectively, which are consistent with the predicted from the modeling. The reported design offers the insights in realizing 2DOF multimode MEMS energy harvester using the piezoelectric ZnO thin films.

Acknowledgements

This research is supported by National Natural Science Foundation of China Grant No. 51705429, National Natural Science Foundation of Shaanxi Province No. 2018JQ5030 and the Fundamental Research Funds for the Central Universities No. 31020170QD070, UK Engineering and Physical Sciences Research Council (EPSRC) EP/P018998/1, Newton Mobility Grant (IE161019) from the UK Royal Society and the National Natural Science Foundation of China, and Royal Academy of Engineering UK-Research Exchange with China and India.

Reference

[1] P. Fang, X. Ma, X. Li, X. Qiu, R. Gerhard, X. Zhang, *et al.* Fabrication, structure characterization, and performance testing of piezoelectret-film sensors for recording body motion, *IEEE Sens. J.* 18(2018) 401-412.

[2] J. Wu, S. Han, T. Yang, Z. Li, *et al.* Highly Stretchable and Transparent Thermistor Based on Self-Healing Double Network Hydrogel, *J. ACS Appl. Mater. Inter.* 10(2018) 19097–19105.

[3] Z. Yang, J. Shi, J. Yao, X. Zhang, G. Ding and X. Zhao, A Laterally Driven MEMS Inertial Switch With Double-Layer Suspended Springs for Improving Single-Axis Sensitivity, *Packag., Manuf. Technol.* 8(2018) 1845-1854.

[4] Y. Liao and J. Liang, Maximum power, optimal load, and impedance analysis of piezoelectric vibration energy harvesters, *Smart Mater. Struct.* 27(2018) 075053.

[5] Y. Yang, Y. Li, Y. Guo, B.-X. Xu, and T. Yang, Improved vibration-based energy harvesting by annular mass configuration of piezoelectric circular diaphragms, *Smart Mater. Struct.* 27(2018) 035004.

[7] K. Tao, J. Wu, A.G.P. Kottapalli, *et al.* Micro-patterning of resin-bonded NdFeB magnet for a fully integrated electromagnetic actuator, *Solid-State Electron.* 138(2017) 66-72.

[8] M. Halim, R. Rantz, Q. Zhang, L. Gu, K. Yang, and S. Roundy, An electromagnetic rotational energy harvester using sprung eccentric rotor, driven by pseudo-walking motion, *Appl. Energy,* 217(2018) 66-74.

[9] H. Liu, S. Gudla, F. A. Hassani, C. H. Heng, Y. Lian, and C. Lee, Investigation of the nonlinear electromagnetic energy harvesters from hand shaking, *IEEE Sens. J,* 15(2016) 2356-2364.

[10] Y. Zhang, T. Wang, A. Luo, Y. Hu, X. Li, and F. Wang, "Micro electrostatic energy harvester with both broad bandwidth and high normalized power density," *Appl. Energy,* 212(2018) 362-371.

[11] G. Chen, Y. Li, H. Xiao, and X. Zhu, "A micro-oscillation-driven energy harvester based on a flexible bipolar electret membrane with high output power," *J. of Mater. Chem. A,* 5(2017) 4150-4155.

[12] K. Tao, J. Wu, L. Tang, L. Hu, S. W. Lye, and J. Miao, Enhanced electrostatic vibrational energy

harvesting using integrated opposite-charged electrets, *J. Micromech. Microeng.* 276(2017) 044002.
[13] Z. L. Wang, J. Chen, and L. Lin, "Progress in triboelectric nanogenerators as a new energy technology and self-powered sensors," *Energ. Environ. Sci.,* 8(2015) 2250-2282.
[14] P. Wang, R. Liu, W. Ding, *et al.* Complementary Electromagnetic - Triboelectric Active Sensor for Detecting Multiple Mechanical Triggering, *Adv. Func. Mate.* 28 (2018) 1705808.
[15] H. Zhang, Y. Lu, A. Ghaffarinejad, and P. Basset, Progressive contact-separate triboelectric nanogenerator based on conductive polyurethane foam regulated with a bennet doubler conditioning circuit, *Nano Energy,* (51)2018 10-18.
[16] B. Yang, Y. Zhu, X. Wang, J.-q. Liu, X. Chen, and C. Yang, High performance PZT thick films based on bonding technique for d31 mode harvester with integrated proof mass, *Sens. and Actuators A: Physical*, 214(2014) 88-94.
[17] R. Elfrink, T.M. Kamel, M. Goedbloed *et al.* Vibration energy harvesting with aluminum nitride-based piezoelectric devices, *J. Micromech. Microeng.* 19(2009) 094005
[18] C. Fei, X. Liu, B. Zhu, D. Li, X. Yang, Y. Yang and Q. Zhou, AlN Piezoelectric Thin Films for Energy Harvesting and Acoustic Devices, *Nano Energ.,* (51)2018, 146-161
[19] B. Zhu, C. Fei, C. Wang, *et al.*, Self-focused AlScN film ultrasound transducer for individual cell manipulation, *ACS sensors*, 2(2017) 172-177
[20] B. Norris, J. Anderson, J. Wager, and D. Keszler, Spin-coated zinc oxide transparent transistors, *J. of Phys. D: Appl. Phys.,* (36)2003, 105
[21] V. L. Patil, S. A. Vanalakar, P. S. Patil, and J. H. Kim, Fabrication of nanostructured ZnO thin films based NO2 gas sensor via SILAR technique, *Sens. and Actuators B: Chemical*, 239(2017) 1185-1193.
[22] P. Wang, H. Du, S. Shen, M. Zhang, and B. Liu, Deposition, characterization and optimization of zinc oxide thin film for piezoelectric cantilevers, *Appl. Surf. Sci.,* (258)2012 9510-9517.
[23] Y.Q. Fu, J.K. Luo, N.T. Nguyen, A.J. Walton, A.J. Flewitt, X.T Zu, Y. Li, G. McHale, A. Matthews, E. Iborra, H. Du, W.I. Milne, Advances in piezoelectric thin films for acoustic biosensors, acoustofluidics and lab-on-chip applications, *Prog. Mater Sci.,* 89 (2017) 31-91.
[24] Y.Q. Fu, J.K. Luo, X. Du, A.J. Flewitt, Y. Li, A. Walton, W.I. Milne, Recent developments in ZnO films for acoustic wave based bio-sensing and microfluidic applications, *Sens. and Actuators B: Chemical,* 143 (2010) 606-619.
[25] Y. Yuan, H. Du, K. S. Chow, M. Zhang, S. Yu, and B. Liu, Performance analysis of an integrated piezoelectric ZnO sensor for detection of head–disk contact, *Microsys. tech.,* (19)2013 1449-1455.
[26] L. Tang, Y. Yang, and C. Soh, Broadband Vibration Energy Harvesting Techniques, in *Advances in Energy Harvesting Methods*, Springer New York, 2013 17-61.
[27] Y. Tadesse, Shujun Zhang, and S. Priya, Multimodal Energy Harvesting System: Piezoelectric and Electromagnetic, *J. Intell. Mater. Syst. and Struct.,* (20)2009 625-632.
[28] Q. Ou, X. Chen, S. Gutschmidt, A. Wood, N. Leigh, and A. F. Arrieta, "An experimentally validated double-mass piezoelectric cantilever model for broadband vibration–based energy harvesting, *J. Intell. Mater. Syst. and Struct.,* (23)2012 117-126.
[29] K. Tao, L. Tang, J. Wu, S.W. Lye, H. Chang, and J. Miao, Investigation of multimodal electret-based MEMS energy harvester with impact-induced nonlinearity, *J. Microelectromech. Syst.,* (27)2018 276-288.

[30] L.C. Zhao, H.X. Zou, G. Yan, W.M. Zhang, Z.K. Peng, and G. Meng, Arbitrary-directional broadband vibration energy harvesting using magnetically coupled flextensional transducers, *Smart Mater. Struct.* 27(2018) 095010.
[31] H. T. Li, W. Y. Qin, J. Zu, and Z. Yang, Modeling and experimental validation of a buckled compressive-mode piezoelectric energy harvester, *Nonlinear Dynam.,* (24)2018 1-20.
[32] S. Zhou and L. Zuo, Nonlinear dynamic analysis of asymmetric tristable energy harvesters for enhanced energy harvesting, *Commun. Nonlinear Sci.* (61)2018 271-284.
[33] W. Tang, L.B. Wang, Y.M. Ren, B. Bao, and J.J. Cao, Design and experimental analysis of self-sensing SSDNC technique for semi-active vibration control, *Smart Mater. Struct.* 27(2018) 085028.